Mineralogical Magazine (2023), **87**, 819–829
doi:10.1180/mgm.2023.82

CAMBRIDGE UNIVERSITY PRESS

Article

Complexity in the Au–Ag–Hg system: New information from a PGE ('osmiridium') concentrate at Waratah Bay, Victoria, Australia

William D. Birch[1] and Chi Ma[2]

[1]Geosciences, Museums Victoria, GPO Box 666 Melbourne, Victoria, Australia and [2]Division of Geological and Planetary Sciences, California Institute of Technology, Pasadena, USA.

Abstract

Au–Hg–Ag phases have been described from a variety of metallogenic orebodies and the placer deposits derived from them. In many documented placer deposits, the phases typically occur intergrown as 'secondary' rims to primary Au–Ag grains. The origin of these rims has been ascribed to supergene redistribution reactions during deposition or to the effects of amalgamation (i.e. use of mercury) during mining for gold. Difficulties in determining compositions and crystal structures on such a small scale have made full characterisation of these phases problematic. This paper describes a new occurrence of these phases, found by accident during investigation of a historical concentrate of 'osmiridium' containing a number of gold grains from beach sands at Waratah Bay, in southern Victoria, Australia. The phases occur as rims to gold grains and are intergrown on a scale of tens of micrometres or less. Application of electron microprobe analysis (EPMA) and limited electron back-scattered diffraction (EBSD) was required to characterise them. These techniques revealed the presence of the approved mineral weishanite (Au–Hg–Ag) and a phase with compositional range Au_2Hg–Au_3Hg surrounding primary Au–Ag (electrum) containing trace amounts of Hg. EBSD analysis showed weishanite is hexagonal $P6_3/mmc$ and Au_2Hg to be hexagonal $P6_3/mcm$. Comparison with published data from other localities (Philippines, British Columbia and New Zealand) suggests weishanite has a wide compositional field. Textures shown by these phases are difficult to interpret, as they might form by either supergene processes or by reaction with anthropogenic mercury used during mining. However, in the absence of any historical evidence for the use of mercury for gold mining at Waratah Bay, we consider the formation of the Au–Hg phases is most probably due to supergene alteration of primary Au–Ag alloy containing small amounts of Hg. In addition to revealing some of the reaction sequences in the development of these secondary Au–Hg–Ag rims, this paper illustrates methods by which these phases can be more fully characterised and thereby better correlated with the Au–Hg synthetic system.

Keywords: Au–Hg–Ag phases; weishanite; EBSD analysis; synthetic Au–Hg system; Waratah Bay; Victoria

(Received 6 June 2023; accepted 21 September 2023; Accepted Manuscript published online: xx xxx; Associate Editor: David J. Good)

Introduction

The discovery of Hg-bearing Au−Ag alloys in an historic 'osmiridium' concentrate from beach sand at Waratah Bay, in southern Victoria, Australia, has prompted a comparison with numerous world-wide occurrences of these enigmatic phases. Many are recorded as overgrowths on gold grains from placer deposits derived from varied geological sources. For example, the approved mineral aurihydrargyrumite (Au_6Hg_5) was found in the Oda River draining through crystalline schists, gabbro and serpentinite in Ehime Prefecture, Shikoku Island, Japan (Nishio-Hamane *et al.*, 2018). In southern New Zealand, alloys with a wide range in composition occur in Quaternary placers derived from sources within the Mesozoic Otago Schist (Youngson *et al.*, 2002). Huang (2011) described Au–Hg phases from placers in the Davao district, Mindanao, Philippines, probably derived from ultramafic–mafic complexes with associated polymetallic deposits. Two hexagonal Au–Hg phases (Au_2Hg and $(Au,Ag)_3Hg_2$) were detected in river placers in western Switzerland (Meisser and Brugger, 2000). Other localities for these alloys in placers include Witwatersrand, South Africa (Oberthür and Saager, 1986); the Snake River, Idaho, USA (Desborough and Foord, 1992); the Tulameen–Similkameen river system in British Columbia, Canada (Barkov *et al.*, 2009); the Inagli deposit in the Aldan Shield, Russia (Svetlitskaya *et al.*, 2018) and in the Palakharya River, Bulgaria (Atanasov and Iordanov, 1983).

Other reports describe Au−Ag−Hg phases from a range of metallogenic deposits. For example, the approved mineral weishanite (Au,Ag,Hg) was discovered in a gold–silver orebody within granulite-facies metamorphic rocks in Henan Province, China, and in the silver–lead orebody in the Keystone Mine, Colorado, USA (Li *et al.*, 1984; Bindi *et al.*, 2018). Other occurrences include the Tsugu Au–Sb vein deposit, Japan (Shikazono and Shimizu, 1988); volcanogenic sulfide deposits at Laangsele, Sweden (Nysten, 1986); at Trout Lake, Manitoba, USA (Healy and Petruk, 1990); and in the Otago Schist quartz-vein deposits of New Zealand (Mackenzie and Craw, 2005). These occurrences indicate these phases can form over a wide range in temperature and sulfur fugacity.

Studies in the synthetic Au–Hg system have characterised a number of stoichiometric phases, such as Au_2Hg, Au_3Hg, Au_6Hg_5 and Au_5Hg_6, known to be stable under 'geologically

Corresponding author: William D. Birch; Email: bbirch@museum.vic.gov.au
Cite this article: Birch W.D. and Ma C. (2023) Complexity in the Au–Ag–Hg system: New information from a PGE ('osmiridium') concentrate at Waratah Bay, Victoria, Australia. *Mineralogical Magazine* **87**, 819–829. https://doi.org/10.1180/mgm.2023.82

reasonable' conditions, i.e. below ~300–400°C (Rolfe and Hume-Rothery, 1967; Okamoto and Massalski, 1989). Of these only Au_6Hg_5 has been formally defined as an approved mineral, aurihydrargyrumite (Nishio-Hamane *et al.*, 2018). Weishanite was originally described as $(Au,Ag)_3Hg_2$ by Li *et al.* (1984), however it was redefined as (Au,Ag,Hg) by Bindi *et al.* (2018). Hexagonal prismatic crystals of Au_3Hg described from Minas Gerais, Brazil by Baptista and Baptista (1987) are likely to be weishanite. The hexagonal Au_3Hg phase from Hunan, China, for which the name 'yiyangite' was proposed by Enkui (1991), has never been approved as a mineral species.

There are a number of difficulties associated with characterising the natural occurrences and correlating them with the synthetic system. These include textural complexity, very small sizes and subtle changes in composition. The prime difficulty is distinguishing between textures that have a purely supergene origin, or those that have involved the influence of mercury for amalgamation during gold mining. Such anthropogenically assisted phases cannot be approved as a mineral species.

Regardless of these difficulties, this paper aims to fully characterise the Waratah Bay Au–Hg–Ag species using a combination of electron back scattered diffraction (EBSD) and electron microprobe analysis (EPMA). Using data from other studies, the Waratah Bay phases are shown to have compositions that differ from other localities, nor do they correlate directly with known synthetic phases, thereby limiting any application to nomenclature in the Au–Ag–Hg system. The reasoning behind preferring an origin by supergene alteration of Au–Ag alloys containing small amounts of Hg, without involvement of anthropogenic Hg is also presented.

The Waratah Bay occurrence

Local prospectors were obtaining detrital gold by traditional panning methods in the beach sands at Waratah Bay, in southern Victoria, Australia, from as early as 1871, although not in sufficient amounts to cause a rush, as had occurred throughout central Victoria from the 1850s. It wasn't until 1915 that the occurrence first came to the attention of mining investors in Melbourne, however, regardless of leases being approved and several companies being registered, there are no records of any large-scale mining taking place. 'Osmiridium' (a general term for Ir–Os alloys) occurring with the gold had only been mentioned in passing in several of the early newspaper reports, as attention focussed instead on the gold. Both the gold and osmiridium are thought to have been derived from a complex belt of faulted and serpentinised Cambrian ultramafic rocks (Maitland Beach Volcanics; Cayley *et al.*, 2002) which crop out for ~5 km along the far south-western margin of the bay (Fig. 1). However, unlike the better known and researched occurrences of platinum-group element (PGE) minerals associated with ultramafic complexes in western Tasmania, there has been no detailed work on the Waratah Bay serpentinites to determine their Au and PGE element contents.

Only one sample of osmiridium has been preserved from the locality, a 35-gram concentrate probably sent to the Victorian Mines Department for assay by an anonymous miner in the late 19th century. It consists almost entirely of osmiridium grains between 1 and 2 mm across, with a few gold grains of similar size. Other minor minerals in the concentrate include quartz, chromite, cassiterite and small red zircons. The presence of these minerals is due to longshore drift in an anti-clockwise direction, bringing the cassiterite from the tin-bearing granite forming Wilsons Promontory to the southeast.

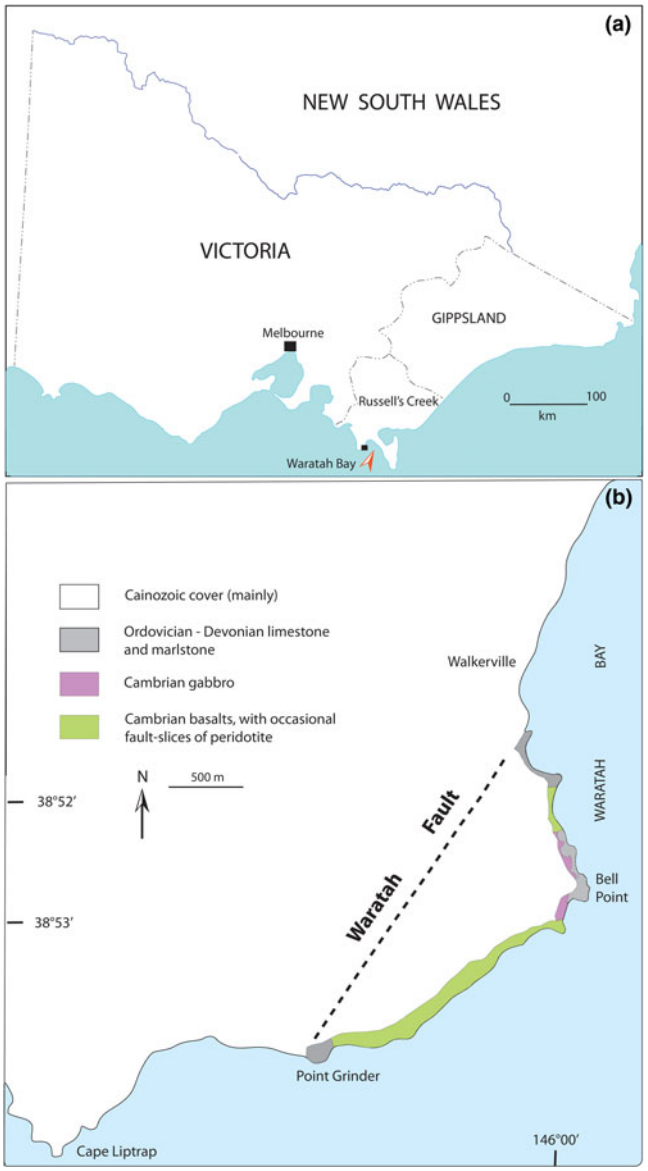

Figure 1. (a,b) Simplified geological and location maps for the Waratah Bay Au–Hg–Ag phases, in Victoria, Australia. The preserved Cambrian source rocks crop out along a narrow coastal strip.

Features of the gold

Historical records described the gold from Waratah Bay as free, coarse, and not water-worn, although in the sample investigated the grains exhibit a range of features, including rounding by abrasion. Generally grains are irregular and up to 2 mm across with dull knobbly surfaces, and partial patinas of iron oxide–hydroxide (Figs 2, 3 and 4). A selection of osmiridium and gold grains were examined by a scanning electron microscope equipped with energy dispersive spectrometry (EDS), in preparation for electron microprobe analysis. Most gold grains were either close to end-member Au or have minor contents of Ag with several grains having detectable Hg. Scanning electron microscopy imagery shows the surfaces of Hg-bearing grains to have a partially etched appearance, with suggestions of crudely hexagonal crystal outlines (Fig. 3b). This texture is remarkably similar to that shown by Hg-bearing gold grains designated as 'Type 2 Au–Ag–

https://doi.org/10.1180/mgm.2023.82 Published online by Cambridge University Press

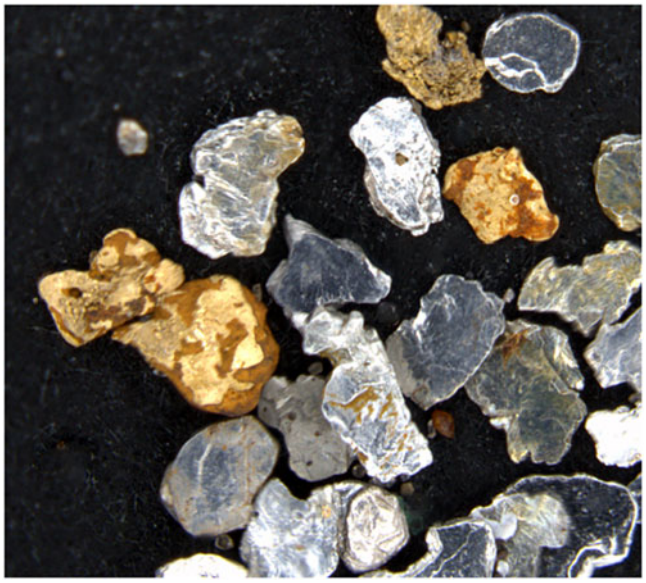

Figure 2. Typical grains of 'osmiridium' and gold (to 2 mm across) in the Waratah Bay concentrate. Gold grains #2 (the larger) and #3 are in contact on the left. Brown areas on these grains are patinas of iron oxides.

Hg alloy' from New Zealand (Youngson *et al.*, 2002, figure 7b) and by aurihydrargyrumite (Nishio-Hamane *et al.*, 2018, Fig. 2c). The appearance suggests progressive removal of Hg along grain boundaries between roughly hexagonal crystals in the surface Au–Hg phase, possibly followed by rounding due to abrasion in the beach sand environment. Two of these Waratah Bay Hg-bearing grains, here designated #2 (Fig. 2) and #20 (Fig. 4), were chosen for further investigation.

Methods

Electron back-scattered diffraction and energy dispersion spectroscopy

Grain #2 was mounted and polished for examination at Caltech (Caltech GPS Division Analytical Facility, California, USA). A ZEISS 1550VP Field-Emission scanning electron microscope

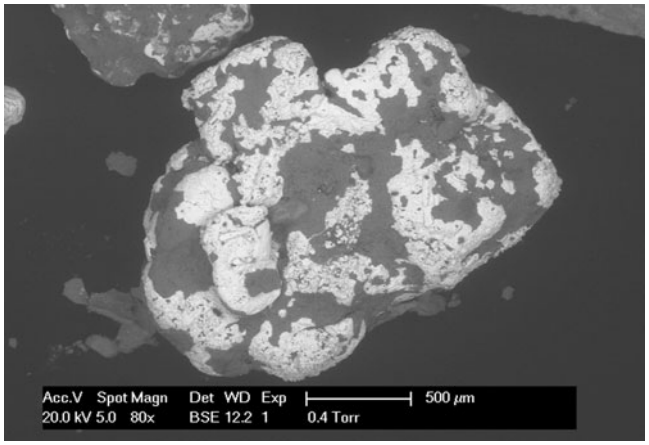

Figure 4. SEM image of grain #20. The dark areas are iron oxide patina.

(SEM) with an Oxford X-Max EDS was used for back-scatter electron (BSE) imaging and elemental analysis. Electron back-scattered diffraction (EBSD) analyses at a submicrometre scale were performed using methods described in Ma and Rossman (2008, 2009). An HKL EBSD system on the ZEISS 1550VP was operated at 20 kV and 6 nA in focused beam mode with a 70° tilted stage and in a variable pressure mode (25 Pa). The EBSD system was calibrated using a single-crystal silicon standard. Structural information was obtained by matching the experimental EBSD patterns with structures of Au, Au–Ag, Au–Hg and Au–Ag–Hg phases from the Inorganic Crystal Structure Database (ICSD, https://icsd.products.fiz-karlsruhe.de/). Back-scattered electron (BSE) imagery revealed a thin prominent marginal alteration zone around the entire grain (Fig. 5). High magnification revealed at least four phases in this marginal zone (Fig. 6a,b). EDS showed that the apparent relict patches in the structure are Au–Ag–Hg, probably weishanite (Fig. 6a, 7a,b), being replaced by a phase with compositions in the range Au_2Hg–Au_3Hg. EBSD (Fig. 8a,b) showed that this phase is hexagonal $P6_3/mcm$, the same as the structure of aurihydrargyrumite. EBSD on another phase appearing to be gradational to the marginal zone showed it to be face-centred cubic, with a composition determined by EDS to be close to $Au_{83}Hg_{17}$ (see Fig. 6b).

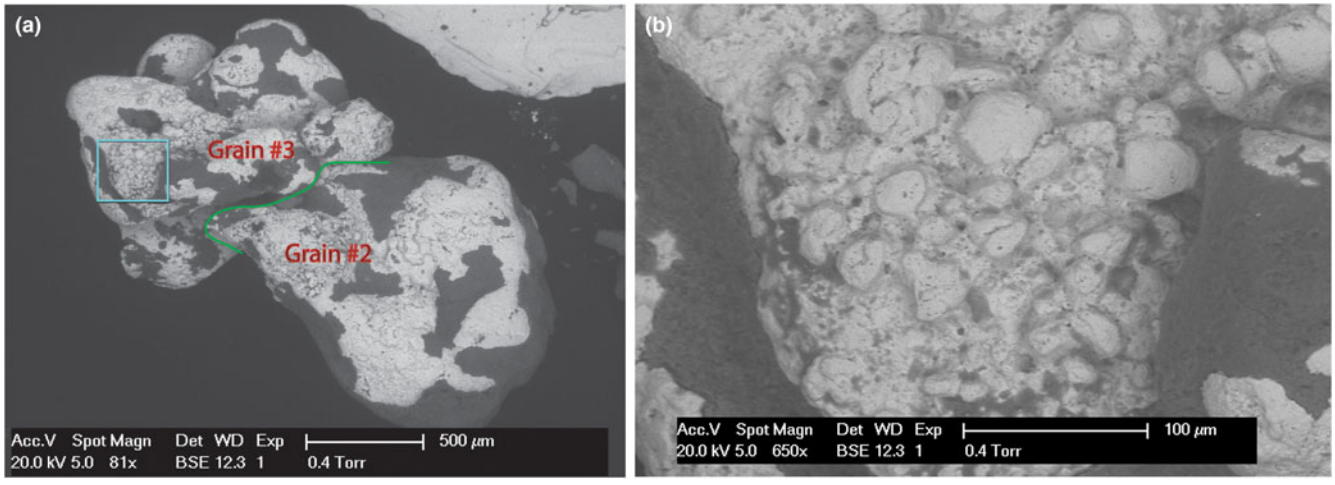

Figure 3. (a) SEM image of gold grains #2 and #3, prior to preparation of a polished section. The dark patches are iron oxide patina. The green line shows the edge of grain #2 overlapping grain #3, and the blue outline shows the area in (b). (b) SEM image of surface texture of Au–Hg phase on grain #3.

https://doi.org/10.1180/mgm.2023.82 Published online by Cambridge University Press

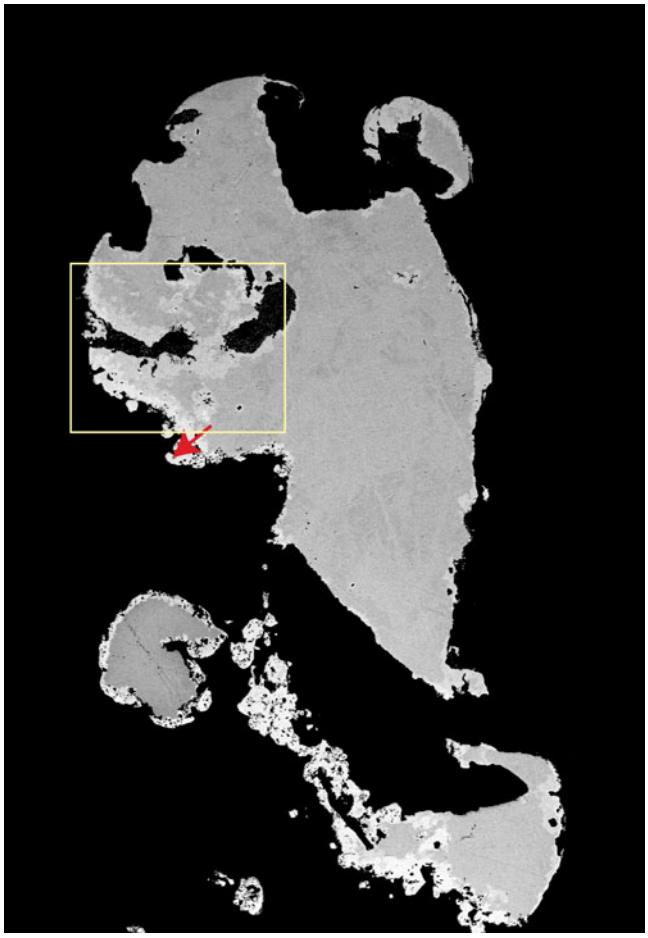

Figure 5. BSE image of Grain #2 polished to show marginal alteration to Au–Hg phases. The red arrow indicates the position of the area shown in Fig. 6a. The yellow box shows the area of Fig. 12. The grain is 2 mm long.

Back-scattered electron imagery of one small area (15 × 11 μm) in this marginal zone (see area outlined on Fig. 6a) showed the irregular patches of weishanite (with a hexagonal $P6_3/mmc$ structure) surrounded by thin mantles of another phase (Fig. 9) which is close to pure gold in composition.

Element distribution images

The area shown in Fig. 9 was selected for X-ray mapping to reveal more detail of the compositional relationship between the weishanite relicts and the surrounding Au–Hg phase. The image for the Ag distribution best shows the weishanite relicts (red) with gold-rich (and Hg-depleted) mantles (yellow to green) grading into the Au–Hg phase (Fig. 10).

Electron microprobe analysis

Grain #20 was mounted and polished for microprobe analysis, using a Joel JXA-830 field emission microprobe in the School of Geography, Earth and Atmospheric Sciences (SGEAS) at the University of Melbourne. Operating conditions in WDS mode were 15 kV, 20 nA, beam diameter 1 μm and with standards of pure Au and Ag, and HgS (cinnabar) for Hg. Overlap of the Au$M\beta$ and Hg$M\alpha$ lines on PET was compensated for by subtracting a proportional amount determined by obtaining the ratio of Au$L\alpha$ counts on the LIF crystal to the Au interference at the Hg position on the PET crystal. This value, 0.007, was then subtracted from the actual Hg peak count before doing the ZAF calculation. This is especially significant for analyses with small amounts of Hg. Detection limits are 90 ppm for Ag and 440 ppm for both Au and Hg. Examination of part of an outer edge of grain #20 using back-scattered electron imaging showed three phases are present, distinguished by differing Au, Ag and Hg contents (Fig. 11). The innermost phase is Au–Ag alloy containing a very small amount of Hg, partly fringed by irregular areas of Au–Hg–Ag, probably weishanite. The outermost phase showing an open framework of roughly hexagonal crystals to 30–40 μm is a Au–Hg alloy with an average composition close to Au_2Hg. (Table 1). Electron microprobe analysis was also undertaken on the phases in part of grain #2 identified at Caltech (Table 1) (Figs 5 and 12). The innermost phase is Au–Ag alloy with minor Hg, surrounded by Au with minor Ag and Hg, with an outer-edge phase of Au–Hg alloy with compositions mostly between Au_3Hg and Au_2Hg (see Fig. 13). The difference between the two is that the middle phase in Fig. 11 is weishanite (Au–Ag–Hg) whereas it's Au with minor Ag and Hg in Fig. 12.

Results and discussion

Compositions

The Waratah Bay electron microprobe data (Table 1) plotted in the Hg–Au–Ag ternary diagram (Fig. 13) have compositions spread along the binary join between Au_2Hg and Au_3Hg, though not extending to Au_6Hg_5. Data points for aurihydrargyrumite and weishanite are also plotted, as well as known synthetic phases along the Au–Hg join. The field boundaries are taken from Youngson *et al.* (2002) who extrapolated them from the Au–Hg and Ag–Hg experimental binary systems, and assuming 25°C. Nearly all published compositions with known crystal structures conform to this scheme, which also includes 'γ-goldamalgam' being cubic (Chen *et al.*, 1981). The exception is the monoclinic symmetry assigned to euhedral crystalline grains with compositions in the range $Au_{94}Hg_6$–$Au_{88}Hg_{12}$ found in placers in Snake River, Idaho, USA (Desborough and Foord, 1992). There is no clear explanation for this anomalous result other than that the grains were heated to 500°C prior to examination by X-ray diffraction. Data for Waratah Bay weishanite cluster in a different position to those of other published descriptions (Bindi *et al.*, 2018; Li *et al.*, 1984) suggesting a wide compositional field. Compositions along the Au–Ag join have Hg contents too low to display on Fig. 13.

Comparison with other localities

Compositional data for Au–Ag–Hg phases from placer deposits in the Philippines, British Columbia (Canada) and South Island (New Zealand) are shown in Fig. 14.

If it is assumed that the weishanite composition can vary, as expressed by the formula (Au,Ag,Hg), these data indicate that aurihydrargyrumite and weishanite occur in the Philippines placers. The British Columbia placers contain weishanite close to the type composition of Bindi *et al.*, (2018), and the New Zealand occurrences (Youngson *et al.*, 2002) are a mix of Au–Ag alloys containing up to ~10 at.% of Hg (Type 1 α-phase, Au–Ag–Hg alloy), possible weishanite and points along the Au–Hg join between Au_2Hg and Au_6Hg_5 (Type 2 Au–Ag–Hg

https://doi.org/10.1180/mgm.2023.82 Published online by Cambridge University Press

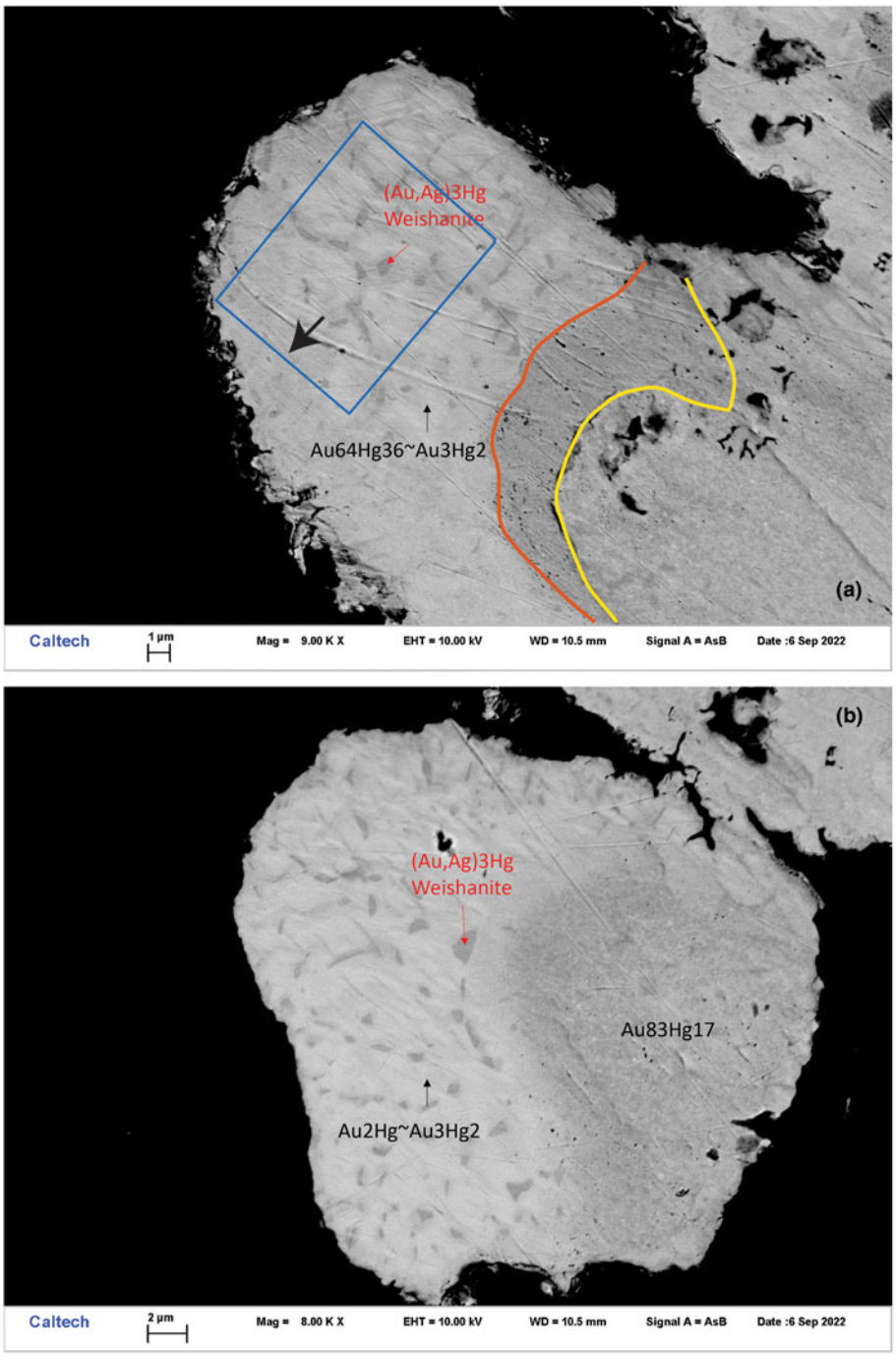

Figure 6. (a,b) Parts of marginal alteration on grain #2 showing texture and formulae obtained by EDS analyses at Caltech. (a) The red and yellow lines mark possible reaction fronts (see text for discussion). The area outlined in blue shows the area and orientation (blue arrow indicates top) of the sample used for Figs 9 and 10. The red arrows in (a) and (b) mark the location of the samples used for EBSD in Figs 7 and 8, respectively.

alloy). The Type 1 phases are ultimately of hydrothermal origin, whereas Type 2 are entirely secondary in origin (Youngson *et al.*, 2002).

Comparison with synthetic phases

Synthetic Au–Hg phases which have close to stoichiometric formulae and for which crystal structure data are known include Au_2Hg, Au_3Hg, Au_4Hg and Au_6Hg_5 (Lindahl, 1970; Rolfe and Hume-Rothery, 1967; Berndt and Cummins, 1970). These, and their mineralogical equivalents, are given in Table 2, adapted from Nishio-Hamane (2018). Attempts to align naturally occurring Au–Hg alloys with synthetic equivalents have proved problematic, mainly because of the wide compositional ranges shown by the natural phases, and the difficulty of obtaining structural data for them. To date the only approved Au–Hg mineral (i.e without Ag) which has a synthetic equivalent is aurihydrargyrumite.

Implications for nomenclature

As shown in Fig. 13, along the Au–Hg join there is essentially a continuous composition between Au_2Hg and Au_3Hg for the Waratah Bay compositions. Au_2Hg has been shown to be hexagonal $P6_3/mcm$ (Berndt and Cummins, 1970), whereas Au_3Hg is $P6_3/mmc$, indicating that somewhere along this compositional interval there is a change in structure from one polytype to

https://doi.org/10.1180/mgm.2023.82 Published online by Cambridge University Press

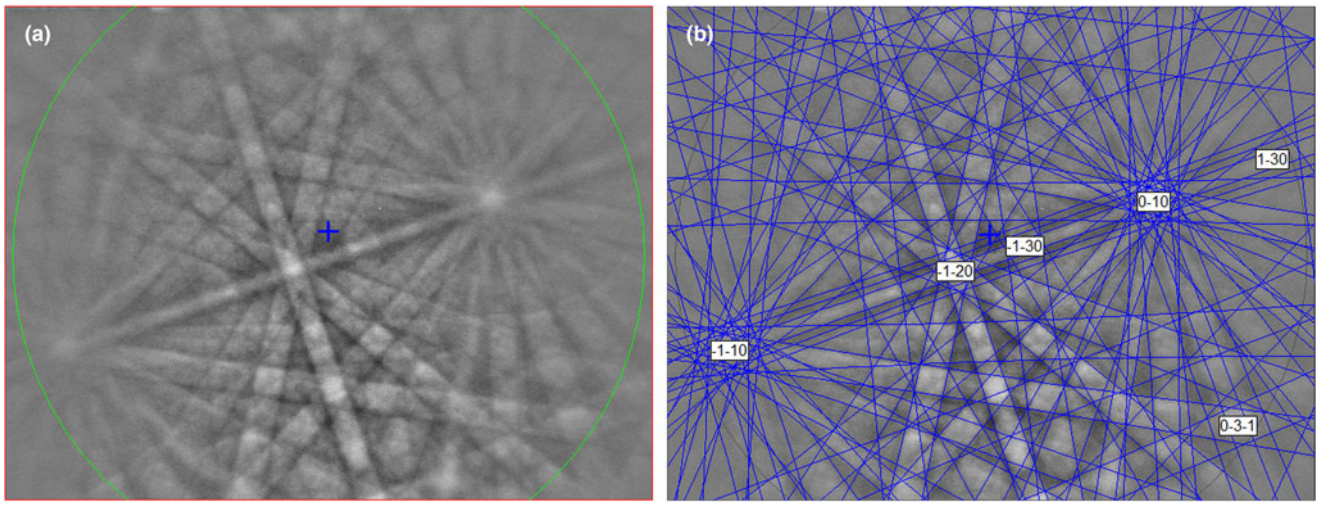

Figure 7. (a) EBSD pattern for weishanite $(Au,Ag)_3Hg$ as shown on Fig. 6a; (b) the pattern indexed with the $P6_3/mmc$ Au_3Hg structure.

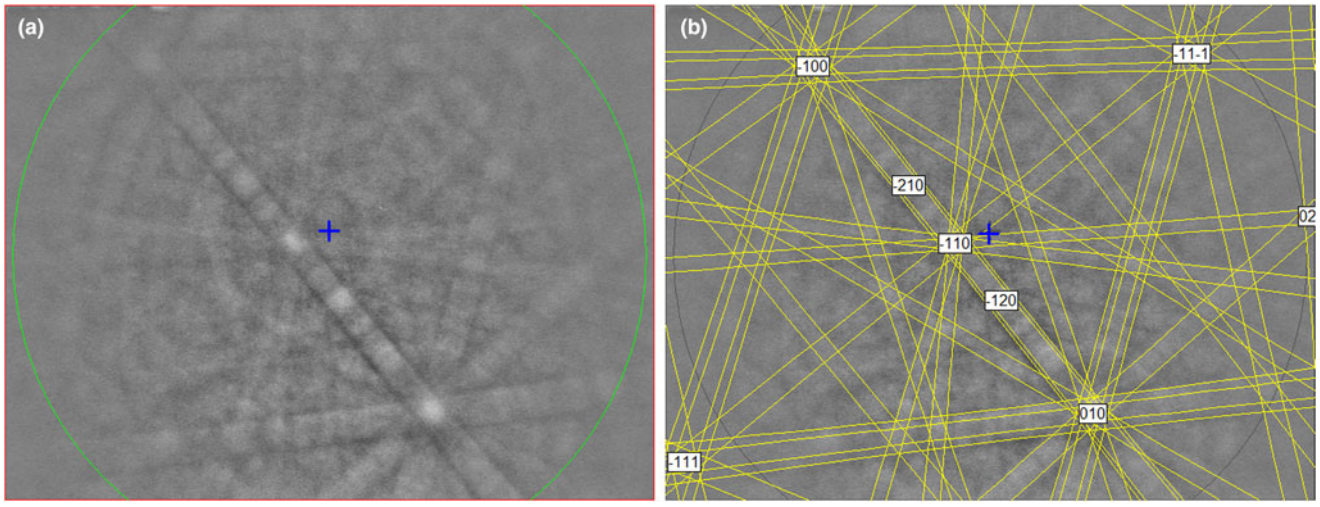

Figure 8. (a) EBSD pattern of Au_2Hg~Au_3Hg_2 as shown on Fig. 6b; (b) the pattern indexed with the $P6_3/mcm$ Au_6Hg_5 structure.

another. It is not possible to determine accurately where this occurs without extremely precise EBSD measurements. However, given that the compositional range encompassing Au_3Hg might be from 21.3 to 25.8 at.% (at 150°C), compared to <1 at.% for Au_2Hg (Rolfe and Hume-Rothery, 1967), the change is probably closer to Au_2Hg.

Although compositional continuity between Au_2Hg and Au_6Hg_5 (aurihydrargyrumite) has not yet been confirmed, both are hexagonal $P6_3/mcm$ (Lindahl, 1970), suggesting that the former might have a wider range in composition. At higher proportions of Hg than aurihydrargyrumite, only cubic 'γ-goldamalgam' has been found naturally, however it has not been sufficiently characterised to have IMA approved mineral status.

In common with Au_3Hg, weishanite is hexagonal $P6_3/mmc$, suggesting the possibility that its compositional field might extend closer to the Au–Hg join near Au_3Hg. Data for weishanite from British Columbia (Fig. 14) plot close to the presumably limiting composition before Ag becomes dominant over Au. As noted by Bindi *et al.* (2018), weishanite is isostructural with schachnerite ($Ag_{1.1}Hg_{0.9}$) (Seeliger and Mücke, 1972), and the two minerals could be considered simple polymorphs of silver and gold, respectively, as the metals are disordered in the same structural position.

Although phases close to Au_2Hg have been reported from a number of localities including in this investigation, it has not been possible to obtain sufficient data to establish it as an IMA approved mineral name, regardless that the crystal structure is known.

Explanation of textures

Based solely on textures in these marginal Au–Hg–Ag phases at Waratah Bay, it is difficult to distinguish between supergene reactions and anthropogenic amalgamation as being responsible for their formation. These overgrowths can be observed in placer deposits where mercury was used to recover gold, but also from sites where there is no evidence for its use. For the latter case, the source of the mercury is the primary gold itself, which might also contain variable Ag contents, i.e. it is a three-phase alloy.

https://doi.org/10.1180/mgm.2023.82 Published online by Cambridge University Press

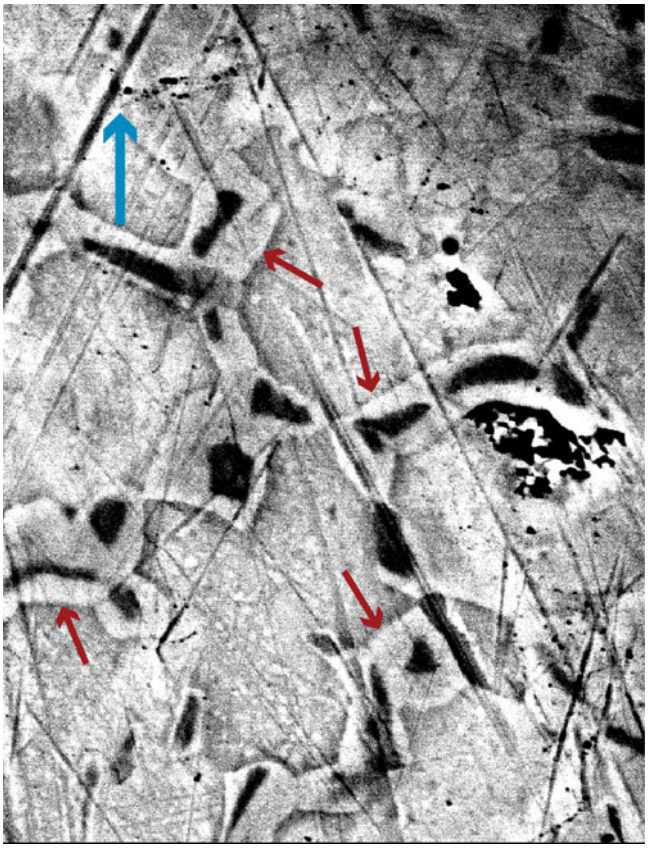

Figure 9. BSE image of area marked on Fig. 6a (blue arrow shows orientation) showing weishanite grains (black) with a gold-rich marginal phase (red arrows). The hosting phase is a Au–Hg alloy.

Several factors need to be considered when deciding on an origin for the Waratah Bay alloys. First, the grains have not been transported a long distance from their possible source i.e. the suite of ultramafic rocks that crop out on the beach where the grains were found. Though some rounding has occurred, this is probably due to wave action affecting the beach sands. Second, there is no strong historical evidence for the use of mercury in the recovery of gold from the beach sands. Third, there are no recorded sources of natural liquid mercury in the region (see below). In combination these three factors suggest an entirely supergene origin for the phases.

Though several features of the grains suggest amalgamation might have occurred, there are other explanations. The morphology of grains #2 and #3 (Fig. 3a) suggests that each might consist of several separate rounded grains which have been amalgamated with Hg. However, another interpretation is that these are rounded, deeply recessed, knobbly grains whose entire margins have been altered with the texture giving the impression there were once separate grains.

Another feature requiring an explanation is the small irregular outgrowths seen, for example in Figs 5, 6a,b. Is it expected that these would not have survived any significant transport, in which case they would only form after the grain had come to rest. This could have been due either to supergene reactions or the effect of amalgamation during collection. However, the nature of the concentrate suggests that traditional panning methods were used to obtain the osmiridium, with the gold grains being accidental additions.

The textures shown in Fig. 6a, b appear to indicate replacement reactions, with two different reaction fronts. In Fig. 6a, one is marked in red and a second one marked in yellow. The region between these interfaces shows a number of pores (dark pores), which are characteristic of a fluid-driven replacement reaction. The area to the left of the red line seems to be a two- or three-phase region which is a mixture of Au_3Hg_2 and $(Au,Ag)_3Hg$. This appears to be an exsolution texture resulting from the solid-state unmixing of a metastable Au–Hg phase. Analogous textures can be seen in the Au–Te system, in which sylvanite is replaced to form calaverite and another phase, which breaks down by exsolution to a mixture of hessite and petzite (Zhao *et al.*, 2013). These can result from supergene hydrothermal reactions, which might occur at ambient temperatures, albeit sluggishly (A. Pring, *pers. comm.*).

Formation of the Au–Ag–Hg phases

The mechanism by which these marginal Au–Ag–Hg phases form in placers is uncertain, with or without, the presence of liquid mercury. Clearly, the phases are secondary and formed under supergene conditions at the expense of primary Au–Ag alloys, which are now preserved in the core of the grains. However, there is considerable disagreement over the mechanism. Youngson *et al.* (2002) attributed the New Zealand occurrences to diffusion between detrital gold grains and liquid Hg that was either hydrothermal in origin or derived from the local breakdown of cinnabar. Barkov *et al.* (2009) favoured an origin for zoned Hg-amalgam as being due to a process of electro-refining involving liquid mercury introduced into the placer deposit, i.e. due to mining operations. Nishio-Hamane *et al.* (2018) explained the formation of aurihydrargyrumite from a Hg component already in the core of the grain and invoked a complex process of ionisation and precipitation, or self-electro-refining, on the surface of gold grains.

Textures revealed by BSE imaging of the Waratah Bay phases provide some evidence for the sequences in which the observed phases have formed. In grain #2, Fig. 6 shows relics of weishanite enclosed in the Au_3Hg–Au_2Hg phase, whereas in Fig. 12, primary Au–Ag–(Hg) is replaced in succession by Au with minor Ag and Hg, in turn replaced at the margins by Au_3Hg–Au_2Hg. For grain #20, a different relationship between the three phases is shown (Fig. 11). It seems clear that the first reaction involved Ag and Hg diffusing towards the margins of the grains, initially forming weishanite. The phenomenon of Ag-depleted rims is commonly observed in Au–Ag grains locked in placer deposits and is broadly described as being due to leaching of silver in supergene environments (Butt *et al.*, 2020). The narrow gold-rich margins observed around relic weishanite in grain #2 (Fig. 9) have not been observed previously, however they appear to be due to a similar process, in which Ag was removed from weishanite, giving rise to the spongy texture observed in the marginal Au–Hg phase. Understandably, the mechanism(s) controlling this process, as well as its timing and environmental conditions, are not well understood and are likely to remain so without considerably more research.

Source of the mercury

The source of both the gold and osmiridium in the Waratah Bay beach sands is considered to be rocks within the Cambrian mafic and ultramafic sequence that crops out along the southwestern coast (Fig. 1b). Although there is no actual evidence for this conclusion, it is supported by the absence of any streams draining

https://doi.org/10.1180/mgm.2023.82 Published online by Cambridge University Press

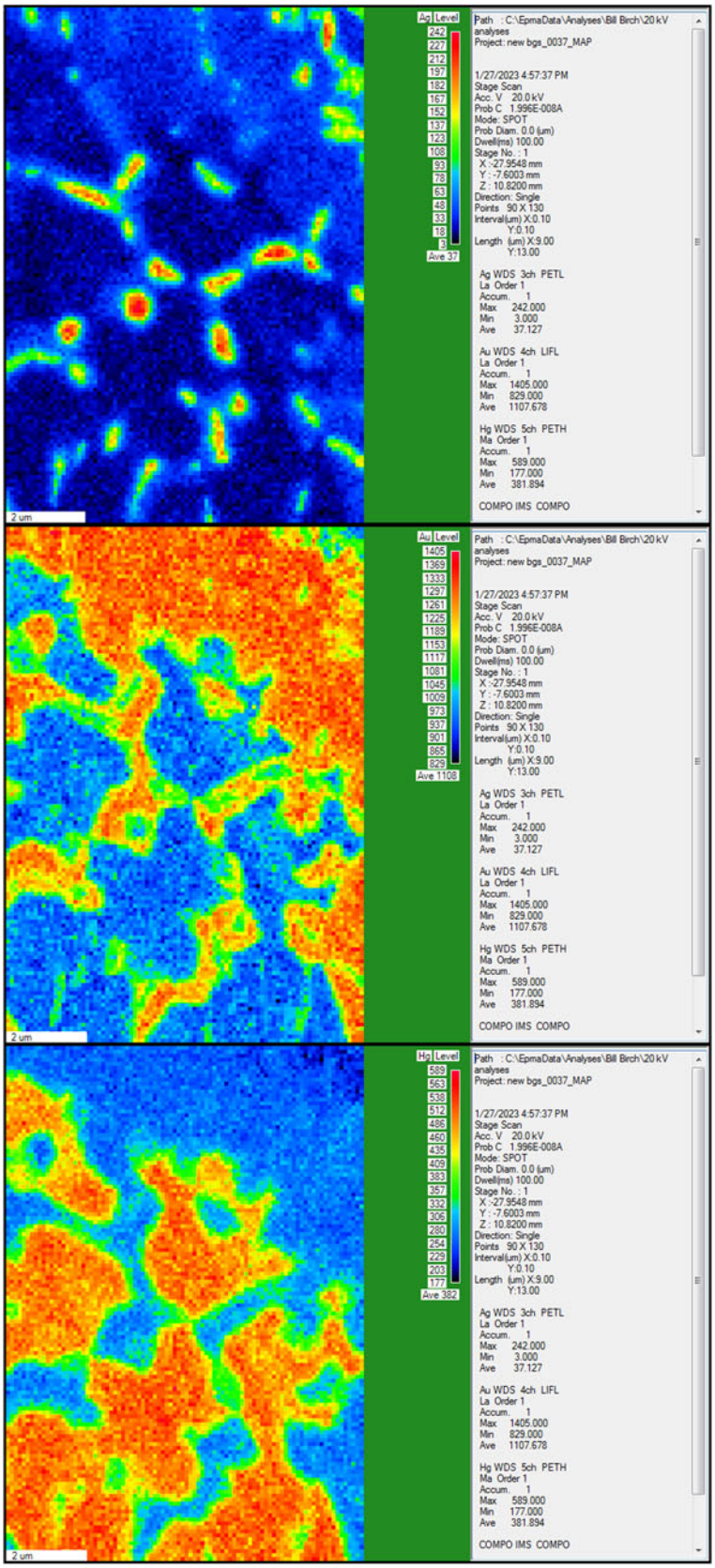

Figure 10. Element-distribution map for Ag (top), Au (middle) and Hg (bottom) for the area shown in Fig. 9 and Fig 6a.

into the bay from known goldfields. As far as is known, this is the only occurrence along the Victorian coast of gold being present in detectable amounts in beach sands.

The Victorian gold province is poor in mercury occurrences, with only one minor deposit known in which liquid mercury and cinnabar occur in quartz veins (Birch, 2003). No data for

https://doi.org/10.1180/mgm.2023.82 Published online by Cambridge University Press

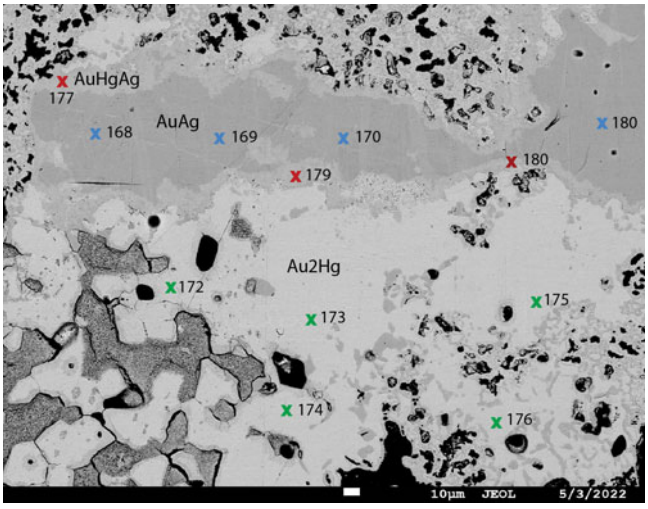

Figure 11. Part of grain #20 showing positions of analysed points on three phases: blue crosses are on Au–Ag alloy with minor Hg; red crosses are on weishanite; and green crosses are on Au–Hg alloy. Numbers refer to analyses in Table 1.

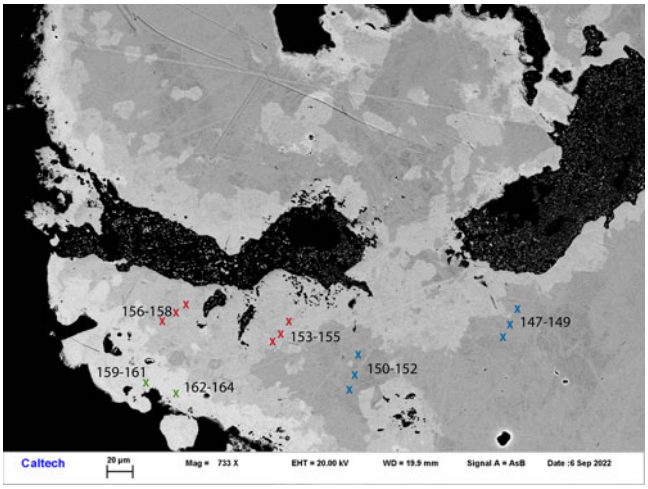

Figure 12. Part of grain #2 (see Fig. 5 for area) showing positions of analysed points on three phases: blue crosses are on Au–Ag alloy with minor Hg; red crosses are on Au with minor Ag and Hg; and green crosses are on Au–Hg alloy. Numbers refer to analyses in Table 1.

Hg contents of natural gold in Victoria appear to exist. Large amounts of mercury were imported into Victoria during the mid-19th century gold rushes to recover gold from pulverised ore and alluvium (placer deposits) by amalgamation (Davies *et al.*, 2015). According to contemporary records published in *Mineral Statistics of Victoria*, an estimated 665 tons of mercury were imported into Victoria between 1868 and 1888. Over that period, the use of mercury (or quicksilver) was recorded for each goldfield in the state. Because of the inefficiency of the amalgamation process, a minimum estimate of 121 tons of mercury were lost from crushing, either flowing into nearby creeks or retained in tailings, with the loss varying from goldfield to goldfield (Davies *et al.*, 2015). Though Waratah Bay was nominally placed in the Russell's Creek mining district in the Gippsland Division, it was not listed as an official goldfield (see Fig. 1a). There are no records of gold production and according to the official records mercury was not used in the Russell's Creek mining district. The possibility of some early prospectors using mercury when panning for gold in the beach sands is remote.

Table 1. Electron microprobe determined compositions of Waratah Bay Au–Hg–Ag phases.

	Weight percent				Atom percent		
No.	Au	Ag	Hg	Total	Au	Ag	Hg
Au–Ag alloy with minor Hg							
Grain #2							
165	77.77	21.92	0.33	100.02	65.84	33.89	0.27
166	79.45	19.89	0.21	99.56	68.50	31.32	0.18
167	76.86	22.14	0.12	99.13	65.46	34.44	0.10
*147	90.47	9.86	0.26	100.59	83.22	16.55	0.23
*148	90.49	9.64	0.28	100.41	83.50	16.24	0.26
*149	90.66	9.40	0.14	100.20	83.97	15.90	0.12
*150	90.42	10.08	0.19	100.69	82.94	16.88	0.17
*151	90.77	10.02	0.16	100.95	83.11	16.74	0.14
*152	90.57	9.98	0.23	100.78	83.07	16.72	0.21
Grain #20							
#168	92.07	8.26	0.36	100.69	85.65	14.03	0.33
#169	92.00	8.56	0.39	100.96	85.17	14.48	0.35
#170	92.64	8.41	0.38	101.43	85.48	14.17	0.35
#171	92.30	8.48	0.40	101.18	85.33	14.31	0.37
Gold with minor Ag and Hg							
Grain #2							
*153	101.16	1.10	0.06	102.32	98.00	1.95	0.06
*154	102.17	0.46	0.02	102.66	99.16	0.82	0.02
*155	101.76	0.33	0.28	102.37	99.15	0.58	0.27
*156	101.55	1.03	0.11	102.69	98.08	1.81	0.11
*157	102.17	0.43	0.16	102.16	99.08	0.76	0.15
*158	101.67	0.86	0.21	102.74	98.27	1.53	0.20
Au–Hg–Ag (weishanite)							
Grain #20							
131	69.64	7.53	20.76	97.93	67.31	13.46	19.23
132	65.49	7.67	25.02	98.18	62.26	13.21	24.53
#177	69.12	7.47	22.85	99.44	65.71	12.96	21.33
#179	70.25	6.89	21.52	98.67	67.57	12.10	20.33
#180	70.48	7.48	20.90	98.86	67.34	13.05	19.61
Au–Hg alloy							
Grain #2							
*159	67.55	0.22	34.13	101.90	66.58	0.39	33.03
*160	72.74	0.12	28.75	101.61	71.88	0.22	27.90
*161	75.53	0.14	25.92	101.59	74.62	0.24	25.14
*162	70.69	0.12	31.33	102.14	69.52	0.22	30.26
*163	71.42	0.28	30.30	102.00	70.24	0.50	29.26
*164	70.83	0.17	31.09	102.09	69.67	0.30	30.03
Grain #20							
#172	70.41	0.35	29.26	100.02	70.55	0.59	28.85
#173	67.00	0.21	32.88	100.09	67.22	0.38	32.39
#174	69.54	0.09	30.56	100.19	69.74	0.16	30.10
#175	69.76	0.16	30.21	100.13	69.95	0.29	29.75
#176	71.02	0.33	29.10	100.45	70.87	0.61	28.52
126	67.28	0.18	32.04	99.53	67.88	0.34	31.80
128	62.54	0.30	36.50	99.34	63.15	0.56	36.25
129	68.80	0.24	30.50	99.54	69.37	0.44	30.19

Footnote:* indicates analysis points shown on Fig. 12; # indicates analysis points shown on Fig. 11.
Formulae for phases determined on Grain #2 by EDS at Caltech are not included

Conclusions

Au–Hg–Ag phases have formed on the margins of several gold grains in beach sands at Waratah Bay, Victoria, Australia. They have similar features and compositions to those present in other placer-gold deposits around the world. Weishanite (Au,Hg,Ag) is the only IMA approved mineral present, however it has a different composition to that from British Columbia, the Philippines and New Zealand. Compositions plotting along the Au–Hg join between Au_3Hg and Au_2Hg do not extend to aurihydrargyrumite

https://doi.org/10.1180/mgm.2023.82 Published online by Cambridge University Press

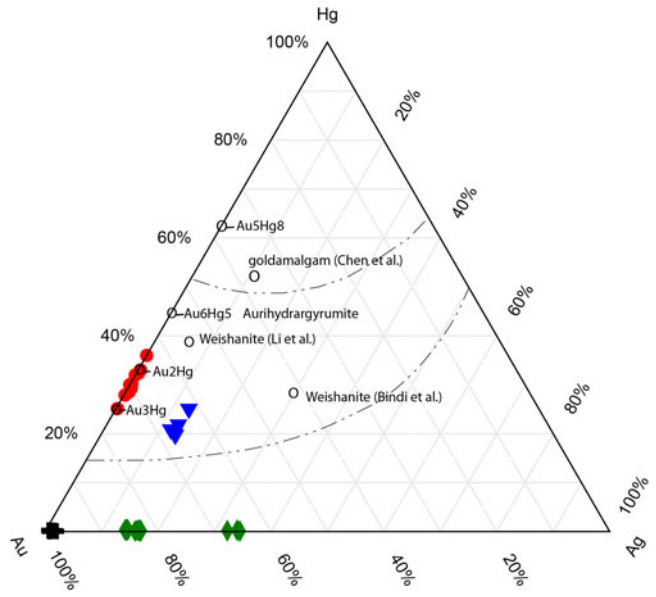

Figure 13. Ternary plot for Waratah Bay mineral data given in Table 1. Red circles are points along the Au–Hg join (Au–Hg alloy in Table 1); blue triangles are interpreted as weishanite; green diamonds are electrum; and black crosses are near-pure gold. Open circles show data for weishanite and aurihydrargyrumite (as defined formally), and for synthetic phases along the Au–Hg join. See text.

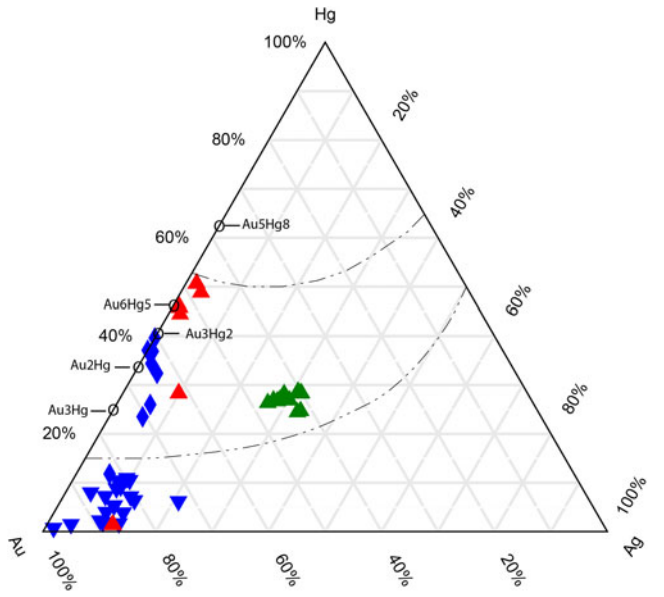

Figure 14. Ternary diagram for analysed Hg–Au–Ag phases from the Philippines (Huang, 2011) (red triangles), British Columbia, Canada (Barkhov *et al.*, 2009) (green triangles) and New Zealand (Youngson *et al.*, 2002) (blue symbols). The blue diamonds are type 2 secondary Au–Ag–Hg alloy and the blue triangles are type 1 (α-phase). Synthetic phases are indicated by open circles.

Table 2. Synthetic phases and their equivalent minerals in the Au–Hg–Ag system.

Phase	Composition (at.% Hg)	Space group	Reference	Equivalent mineral	Mineral reference
Au	0 to 19.8	$Fm\bar{3}m$		Gold	
Au_3Hg	21 to 26	$P6_3/mmc$	Okamoto and Massalski (1989)	'Yiyangite'	Enkui (1991)
Au_2Hg	33.3	$P6_3/mcm$	Berndt and Cummins (1970)	None approved	
Au_6Hg_5	45.5	$P6_3/mcm$	Lindahl (1970)	Aurihydrargyrumite	Nishio-Hamane *et al.* (2018)
Au_5Hg_8	61.5	$I\bar{4}3$	Plaksin (1938)	None approved	
(Au,Ag,Hg)	Variable	$P6_3/mmc$		Weishanite	Li *et al.* (1984); Bindi *et al.* (2018)
(Au,Ag)Hg		$Im3m$	–	'γ-gold amalgam'	Chen *et al.* (1981)

(Au_6Hg_5) and do not represent accepted species. High-magnification X-ray imagery shows a complex assemblage of phases formed as weishanite is resorbed to form the marginal Au–Hg phase simultaneously with leaching of Ag to the environment. In the absence of any historical evidence for the use of mercury to recover gold, it is probable that the marginal Au–Hg phases at Waratah Bay have formed from primary Au–Ag alloys (in some cases electrum) containing minor amounts of Hg, by a process which is not well understood, but which might involve supergene replacement reactions. These phases are further evidence for the complexity of the natural Au–Hg–Ag system and the difficulty involved in refining their nomenclature. Methods such as detailed EBSD combined with precise EPMA are required to understand completely the Au–Ag–Hg system.

Acknowledgements. Graham Hutchinson (University of Melbourne's School of Geography, Earth and Atmospheric Sciences) is thanked for the electron microprobe data and SEM and BSE imagery. SEM-EBSD analyses were carried out at the Caltech GPS Division Analytical Facility, which is supported, in part, by NSF Grants EAR-0318518 and DMR-0080065. Oskar Lindenmayer (Museums Victoria) carried out photography and assisted with drafting.

Competing interests. The authors declare none.

References

Atanasov V. and Iordanov L. (1983) Amalgams of gold from the Palakharya River alluvial sands, District of Sofia (Bulgaria). *Doklady Bolgarskoi Akademii Nauk*, **36**, 465–468.

Baptista N.R. and Baptista A. (1987) Gold amalgam, a possible new species, from Sumidouro de Mariano, Minas Gerais (Brazil). *Anais da Academia Brasileira de Ciencias*, **58**, 457–463 [in Portuguese].

Barkov A.Y., Nixon G.T., Levson V. and Martin R.F. (2009) A cryptically zoned amalgam $(Au_{1.5–1.9}Ag_{1.1–1.4})_{\Sigma 2.8–3.0}Hg_{1.0–1.2}$ from a placer deposit in the Tulameen–Similkameen river system, British Columbia, Canada: natural or man-made? *The Canadian Mineralogist*, **47**, 433–440.

Berndt A.F. and Cummins J.D. (1970) The crystal structure of the Au_2Hg phase. *Acta Crystallographica*, B26, 864–867.

Bindi L., Keutsch F.N. and Lepore G.O. (2018) Structural and chemical study of weishanite, (Au,Ag,Hg), from the Keystone mine, Colorado, USA. *Mineralogical Magazine*, **82**, 1141–1145, doi.org/10.1180/mgm.2018.113

Birch W.D. (2003). The Jamieson mercury deposit, Victoria. *Australian Journal of Mineralogy*, **9**, 33–38.

Butt C.R.M., Hough R.M. and Verrall M. (2020) Gold nuggets: the inside story. *Ore and Energy Resource Geology*, 4–5, 100009 [viewed online on 17/5/2017].

Enkui Cao (1991) The discovery and research of yiyangite in the Hanjiang River. *Geology of Shannai*, **91**, 89–92 [in Chinese with English abstract].

Cayley R.A., Taylor D.H., VandenBerg A.H.M. and Moore D.H. (2002) Proterozoic – Early Palaeozoic rocks and the Tyennan Orogeny in central Victoria: The

Selwyn Block and its tectonic implications. *Australian Journal of Earth Sciences*, **49**, 225–254, https://doi.org/10.1046/j.1440-0952.2002.00921.x

Chen K., Yang H. Ma L. and Peng Z. (1981) The discovery of two new minerals — γ-goldamalgam and leadamalgam. *Dizhi Pinglum*, **27**, 107–115 [in Chinese with English abstract; summary in: New mineral names. *American Mineralogist*, 70, 214–221 (1985)].

Davies P., Lawrence S. and Turnbull J. (2015) Mercury use and loss from gold mining in nineteenth-century Victoria. *Proceedings of the Royal Society of Victoria*, **127**, 44–54.

Desborough G.A. and Foord E.E. (1992) A monoclinic, pseudo-orthorhombic Au–Hg mineral of potential economic significance in Pleistocene alluvial deposits of southeastern Idaho. *The Canadian Mineralogist*, **30**, 1033–1038.

Healy R.E. and Petruk W. (1990) Petrology of the Au–Ag–Hg alloy and "invisible" gold in the Trout Lake massive sulphide deposit, Flin Flon, Manitoba. *The Canadian Mineralogist*, **28**, 189–206.

Huang S. (2011) Mineralogical characteristics of gold–mercury mineral in the Davao gold deposits of Mindanao Islands, Philippines, and its prospecting significance. *Geology and Exploration*, **47**, 935–942 [in Chinese with English abstract].

Li Y., Ouyang S. and Tian P. (1984) Weishanite – a new gold-bearing mineral. *Acta Mineralogica Sinica*, 4, 102–105 [in Chinese with English abstract].

Lindahl T. (1970) The crystal structure of Au_6Hg_5. *Acta Chemica Scandinavica*, **24**, 946–952.

Ma C. and Rossman G.R. (2008) Barioperovskite, $BaTiO_3$, a new mineral from the Benitoite Mine, California. *American Mineralogist*, **93**, 154–157.

Ma C. and Rossman G.R. (2009) Tistarite, Ti_2O_3, a new refractory mineral from the Allende meteorite. *American Mineralogist*, **94**, 841–844.

Mackenzie D.J. and Craw D. (2005) The mercury and silver contents of gold in quartz vein deposits, Otago Schist, New Zealand. *New Zealand Journal of Geology and Geophysics*, **48**, 265–278.

Meisser N. and Brugger J. (2000) Alluvial native gold, tetraauricupride and $AuSn_2$ from Western Switzerland. *Schweizerische Mineralogische und Petrographische Mitteilungen*, **80**, 291–298.

Nishio-Hamane D., Tanaka T. and Minakawa T. (2018) Aurihydrargyrumite, a natural Au_6Hg_5 phase from Japan. *Minerals*, **8**, 415, doi:10.3390/min8090415

Nysten P. (1986) Gold in the volcanogenic mercury-rich sulfide deposit Langsele, Skellefte ore district, northern Sweden. *Mineralium Deposita*, **21**, 116–120.

Oberthür T and Saager R. (1986) Silver and mercury in gold particles from the Proterozoic Witwatersrand placer deposits of South Africa: metallogenic and geochemical implications. *Economic Geology*, **81**, 20–31.

Okamoto H. and Massalski T.B. (1989) The Au–Hg (gold-mercury) system. *Bulletin of Alloy Phase Diagrams*, **10**, 50–58.

Plaksin I.N. (1938) The system gold-mercury. *Izvestiya Sektora fiziko-khimicheskogo Analiza*, **10**, 129–159 [in Russian].

Rolfe C. and Hume-Rothery W. (1967) The constitution of alloys of gold and mercury. *Journal of less-common metals*, **13**, 1–10.

Seeliger E. and Mücke A. (1972) Para-schachnerit, $Ag_{1.2}Hg_{0.8}$, und schachnerit, $Ag_{1.1}Hg_{0.9}$, vom Landsberg bei Obermoschel, Pfalz. *Neues Jahrbuch für Mineralogie Abhandlungen*, **117**, 1–18.

Shikazono N. and Shimizu M. (1988) Mercurian gold from the Tsugu gold-antimony vein deposit in Japan. *The Canadian Mineralogist*, **26**, 423–428.

Svetlitskaya T.V., Nevolko P.A., Kolpakov V.V. and Tolstykh N.D. (2018) Native gold from the Inagli Pt-Au placer deposit (the Aldan Shield, Russia): geochemical characteristics and implications for possible bedrock sources. *Mineralium Deposita*, **53**, 323–338.

Youngson J.H., Woperis P., Kerr L.C. and Craw D. (2002) Au–Ag–Hg and Au–Ag alloys in Nokomai and Nevis valley placers, northern Southland and Central Otago, New Zealand, and their implications for placer-source relationships. *New Zealand Journal of Geology and Geophysics*, **45**, 53–69.

Zhao J., Brugger J., Xia F., Ngothai Y., Chen G. and Pring A. (2013) Dissolution-reprecipitation v. solid-state diffusion: mechanism of mineral transformation in sylvanite $(AuAg)_2Te_4$ under hydrothermal conditions. *American Mineralogist*, **98**, 19–32.

https://doi.org/10.1180/mgm.2023.82 Published online by Cambridge University Press